Measurement of the photoelectric cross section of H_2 at 5.4 and 8.4 keV*

Bernd Crasemann, Paul E. Koblas,† Ta-Cheng Wang, Harvey E. Birdseye, and Mau Hsiung Chen
Department of Physics, University of Oregon, Eugene, Oregon 97403
(Received 23 April 1973; revised manuscript received 23 October 1973)

The photoelectric cross section of molecular hydrogen has been measured by counting photoelectrons released by monochromatized x rays traversing highly purified H_2 gas. Results are 54.0 ± 2.9 mb/atom at 5.41 keV and 12.0 ± 0.6 mb/atom at 8.39-keV incident-photon energy. The effect of molecular bonding is pronounced: The measured cross section, per atom, exceeds the theoretical *atomic* cross section by (44 ± 8)% at 5.41 keV and by (45 ± 7)% at 8.39 keV. A comparable effect has been predicted by Kaplan and Markin.

I. INTRODUCTION

Previous experiments on the attenuation of x rays by hydrogen have been based on absorption-cell techniques. Gaseous samples,[1-5] paraffin,[6] and H_2O_2 in water[7] have been employed. The results are reasonably consistent, as indicated in Fig. 1, where we have plotted measured total photon attenuation cross sections for H_2 in the range from 100 eV to 200 keV. The curve derived by Veigele *et al.*[8a] from a critical evaluation of experimental data is also shown.

Above 1-keV photon energy, it is difficult to derive accurate photoelectric cross sections from the measured total attenuation cross sections, because coherent and incoherent scattering compete with the photoelectric process in a very energy-dependent fashion (Fig. 2). Thus the subtraction of theoretical scattering cross sections from measured total cross sections leads to widely spread results (Fig. 3). This uncertainty is reflected in the differences (by as much as a factor of 5) between hydrogen photoelectric cross sections listed in older tabulations based on such semiempirical results[8a,9a] and on theory alone[10,11] (Fig. 4). In the latest revisions of these tabulations,[8b,9b] theoretical photoelectric H_1 cross sections have been substituted for the earlier semiempirical values.

Better knowledge of H_2 photoelectric cross sections in the keV region is of interest as a guide to theoretical work and in applications. For example, these cross sections are essential for the interpretation of stellar x-ray spectra[12]; photoelectric cross-section ratios $\sigma(H_2)/\sigma(He)$ ranging from 0.2 to 0.8 have been used in calculations of the interstellar absorption of cosmic x rays.[13-15]

In the present paper we describe a direct measurement of the photoelectric cross section of H_2 molecules based on the counting of individual photoelectrons released by x rays that traverse very pure hydrogen gas.

II. EXPERIMENT

A. Principle

Characteristic lines from the target of an x-ray tube are selected by means of a crystal-diffraction spectrometer. The monochromatized and tightly collimated photon beam passes coaxially through a specially designed proportional counter filled with highly purified hydrogen gas (Fig. 5). The active region of the proportional counter is defined electrostatically by means of field tubes; photoelectrons released in this region are attracted to the vicinity of the anode wire, where multiplication takes place. Compton electrons are of much lower energy, so they do not contribute to the photoelectron peak in the proportional-counter spectrum. Photoelectrons released by scattered photons which impinge upon the wall of the proportional counter are degraded in energy by a retarding field between the counter wall and a grid which serves as the cathode. Photoelectrons ejected from the beryllium entrance and exit windows of the proportional counter cannot reach the active region, because their range is very much shorter than the distances between the windows and the edges of the active volume. The intensity of the beam leaving the proportional counter is monitored.

B. Apparatus

The shell of the hydrogen proportional counter consists of a 17.8-cm-i.d. 36.8-cm-long aluminum tube (Fig. 5). Field-tube assemblies are mounted on each end cap; they project 8.4 cm into the counter. The center wire of 0.05-mm-diam stainless steel is shielded from the field tubes by grounded guard tubes. The cathode is a 15.2-cm-diam coaxial cylindrical grid which consists of 75 equally spaced 0.25-mm-diam stainless-steel wires; a 0.6–2-kV retarding potential between the

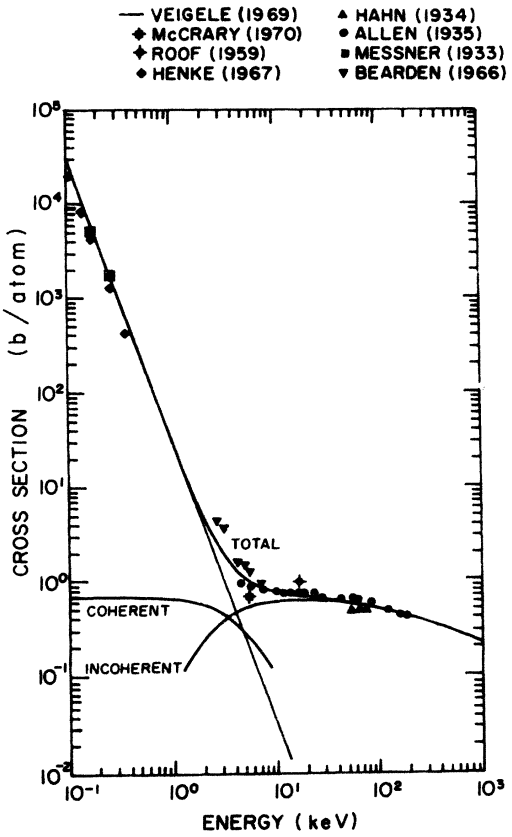

FIG. 1. Measured total x-ray cross sections for hydrogen, after Refs. 1–7. The curve labeled "total" has been derived by Veigele *et al.* (Ref. 8a) from critically evaluated experimental data; scattering cross sections indicated by the curves labeled "coherent" and "incoherent" were calculated from theory (Ref. 8a).

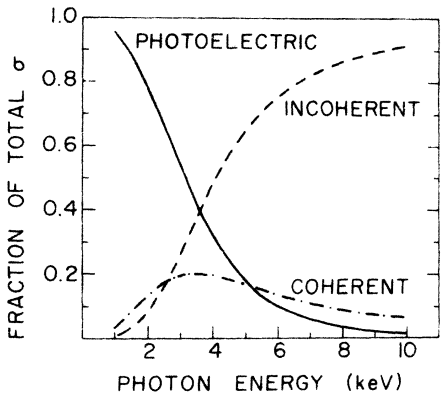

FIG. 2. Fractions of the total x-ray cross section of hydrogen which are due to the photoelectric effect, coherent scattering, and incoherent scattering, according to Storm and Israel (Ref. 9).

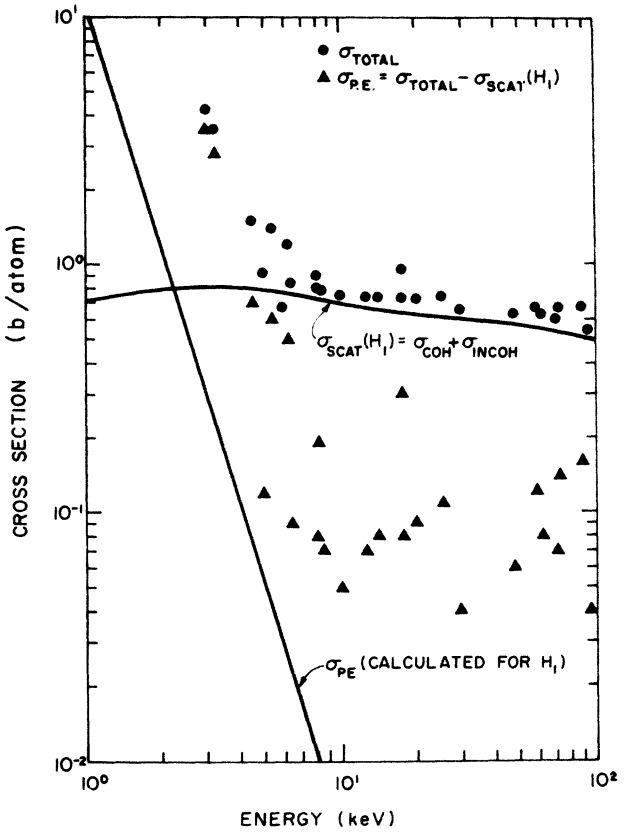

FIG. 3. Photoelectric cross sections of H_2 as determined by subtracting theoretical scattering cross sections according to Veigele *et al.* (Ref. 8) from measured total cross sections (Refs. 2, 3, 5, and 6). The calculated photoelectric cross section for hydrogen atoms is shown for comparison.

cathode and the counter shell degrades photoelectrons that could be ejected from the aluminum wall by scattered x rays.

The x rays enter and leave through glass beam tubes capped with 0.127-mm-thick beryllium windows; the beam axis is parallel to the center wire, at a distance of 4.8 cm from it. Seals are neoprene *O*-rings, separated by indium gaskets from the counter gas. Spacers and insulators are made of glass and ceramics.

The center wire is maintained near ground potential. The cathode potential is approximately -2900 V for 760-Torr H_2 pressure and -4300 V for 1500-Torr pressure. The field tubes are placed at the potential which would exist at their radius in an infinitely long counter.[16] Then the electric field lines in the counter are strictly radial, and the active region is sharply defined by the 19.8-cm distance between field-tube ends.

X rays are generated by commercial 3000-W water-cooled tubes with Cr or W anodes. Char-

acteristic lines (Cr$K\alpha$ or W$L\alpha$) from the target are selected by a goniometer equipped with a LiF crystal and 0.4° Soller slits for angular definition. The beam is further collimated by a 0.15° Soller-slit assembly oriented at 90° to the exit slit. The beam spread is 8.0×10^{-3} rad in the horizontal plane and 1.4×10^{-3} rad vertically; the diameter of the beam is 1.0 cm at a distance of 150 cm from the collimator.

Two alternative beam-flux monitoring devices are used. One, illustrated in Fig. 5, permits counting of fluorescent radiation from a thin foil inserted in the x-ray beam. The second device consists of an arrangement of carefully calibrated and accurately positioned absorber foils which attenuate the beam to a level at which it can be counted with a scintillation or Xe-filled proportional counter (Sec. II C).

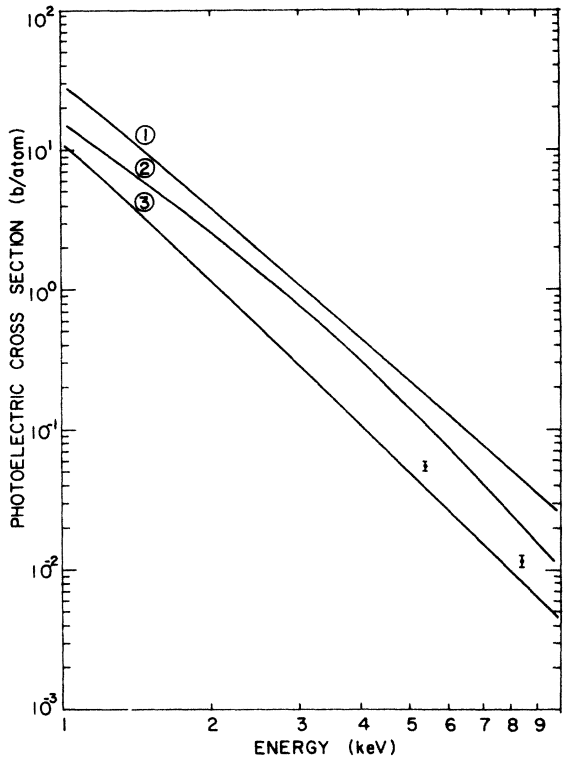

FIG. 4. Hydrogen photoelectric cross sections as a function of photon energy. Values derived by subtracting theoretical scattering cross sections from measured total absorption cross sections form the basis for the older tabulations by Veigele *et al.* (Ref. 8a, curve 1) and Storm and Israel (Ref. 9a, curve 2). Theoretical atomic cross sections (curve 3) are listed in the compilations of McMaster *et al.* (Ref. 10), Plechaty and Terrall (Ref. 11), and in the latest revisions of the tables of Veigele *et al.* (Ref. 8b) and of Storm and Israel (Ref. 9b). The data points at 5.4 and 8.4 keV are the measured H_2 photoelectric cross sections (per atom) from the present work.

Very high gas purity is essential because of the smallness of the H_2 photoelectric cross section, which is four orders of magnitude smaller than that of nitrogen, for example. Traces of impurities can therefore lead to excessive measured cross sections. In this experiment the helium leak-tested apparatus was filled with ultra-high-purity (UHP) hydrogen[17] through a Pd-Ag alloy hydrogen diffusion purifier; this process has been found[18] to reduce the impurity content to below a few parts in 10^{10}. Gas pressure was measured with a Heise 0–3800-Torr Bourdon-tube pressure gauge of accuracy ±3.8 Torr.

Pulses from the hydrogen proportional counter were processed through a field-effect transistor (FET) preamplifier, linear amplifier, and baseline restorer, and recorded in a 512-channel analyzer. Similar standard electronics and a second multichannel analyzer were connected with the beam-monitoring devices.[19]

C. Operation and procedure

1. *Alignment*

For the purpose of alignment the beryllium windows were removed from the beam path and the LiF diffraction crystal was replaced with a front-silvered mirror; a laser beam was used to adjust all components so that the beam axis coincided with the centers of windows and beam tubes. Alignment of the x-ray beam was verified photographically at intervals throughout the experiment. Crossed wires were mounted at the entrance and exit windows of the hydrogen proportional counter and at the beam-monitor exit port, and Polaroid Type 57 film was exposed in the latter location. The image of the beam on the film showed that the <1.0-cm-diam beam was centered in the 2.5-cm-i.d. beam tube. Typical images of the beam (without cross wires) are shown in Fig. 6.

2. *Gas purity*

The gas-filling system[19] and counter were prepared by prolonged evacuation and flushing with diffusion-purified hydrogen for more than one week. The flushing rate was in excess of one detector volume per hour. To avoid possible contamination of the hydrogen by outgassing of counter components, measurements at ~760 Torr were conducted mostly in the flow mode, continually passing ~1 cm^3/sec of diffusion-purified hydrogen through the counter. Measurements at other than atmospheric pressures were made immediately after prolonged vigorous flushing.

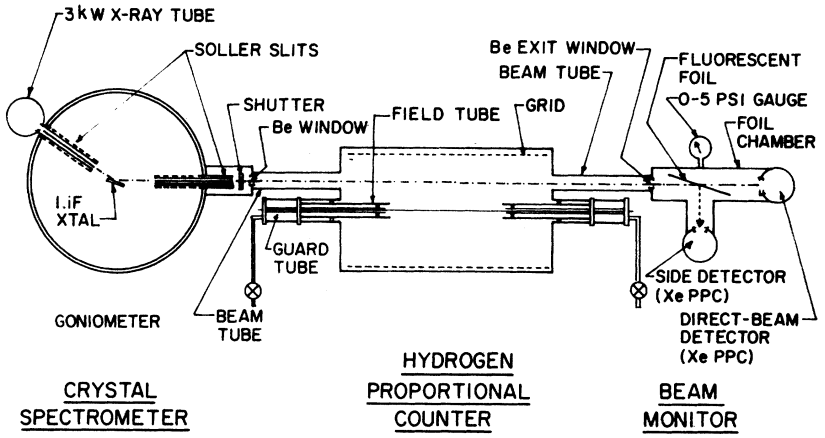

FIG. 5. Schematic representation of experimental apparatus, with one of two alternative beam-monitoring arrangements.

Photoelectric cross sections at 5.41 keV measured with commercial UHP hydrogen[17] that had not been taken through the Pd-Ag diffusion purifier exceeded results from diffusion-purified gas by 7%. The manufacturer indicates that this gas has been produced from liquid-hydrogen boil-off. Impurities, due to air contamination during the cylinder filling operation, are listed by the manufacturer as <1 ppm oxygen, <4 ppm nitrogen, and <2 ppm water. Batch analysis also indicates <50 ppm helium. Other impurities are expected to be present in proportion to their concentration in air. For example, 1% argon in the atmosphere yields 0.05 ppm argon in the gas sample. From tabulated cross sections,[8] the impurities in the UHP hydrogen contribute a calculated $\lesssim 7.8\%$ to the effective photoelectric cross section of the UHP gas, in agreement with the measured difference of 7% between the cross sections of this sample and of diffusion-purified hydrogen. We infer that the latter gas does indeed contain only a negligible amount of impurities.

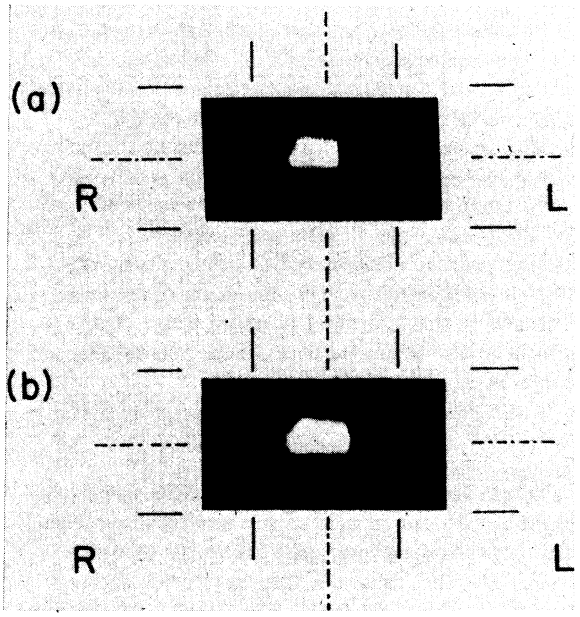

FIG. 6. Images of collimated Cr $K\alpha$ x-ray beam, (a) at entrance window and (b) at exit window of hydrogen chamber. Polaroid Type 57 film was exposed for (a) 210 min and (b) 240 min. Position of the edges of the 2.54-cm-diam beryllium windows is indicated by solid lines; the dot-dash lines intersect at the window centers.

3. *Operating characteristics of H_2 proportional counter*

Well-defined photopeaks could be obtained from the proportional counter over a hydrogen-pressure range from 100 to 1500 Torr, the limit set by the strength of the beryllium windows. A typical spectrum is illustrated in Fig. 7(a). Consistency of cross sections measured at different pressures indicates that electron attachment[20] does not noticeably affect the photoelectron-collection and gas-multiplication processes in this system.

Proper adjustment of the field-tube voltage results in a symmetric photopeak [Fig. 7(a)]. In the present apparatus the optimum field-tube potential is 70% of the cathode potential. When the field-tube voltage is increased to 75% of the cathode voltage, the photopeak begins to show a high-energy tail, and the measured photoelectron production rate increases by 2%; with the field tubes at 80% of the cathode potential, a very pronounced high-energy tail on the photopeak and an increase of 7% in the measured photoelectron production rate is observed. The increased photoelectron production can be ascribed to a lengthening of the active counter volume at the radius of the x-ray beam, due to the fact that the electric field lines

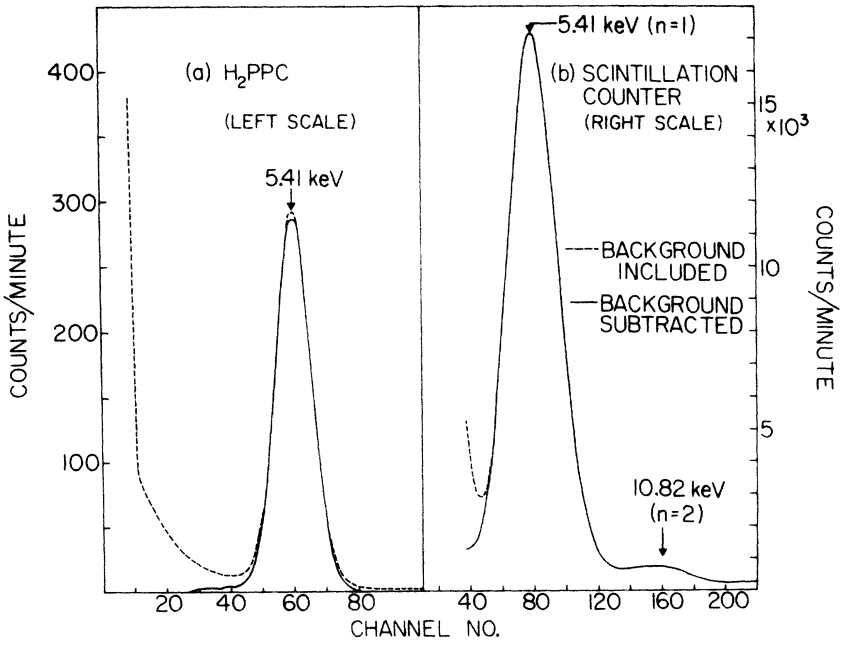

FIG. 7. (a) Pulse-height spectrum of Cr $K\alpha$ x rays, measured with the proportional counter filled with hydrogen to 761 Torr. Cathode potential −2900 V, shell −2300 V, field tubes −2030 V. Counting time 40 min. (b) Scintillation spectrum from beam monitor, same run. The Cr $K\alpha$ x rays have been attenuated by a factor of ~64 by Al absorbers. The second-order diffraction peak at 10.8 keV is made relatively more prominent by the absorbers; in the beam traversing the hydrogen chamber, the intensity of 10.8-keV photons is ≤0.1% of the Cr $K\alpha$ intensity. The Cr-anode x-ray tube was operated at 50 kV and 40 mA during this run.

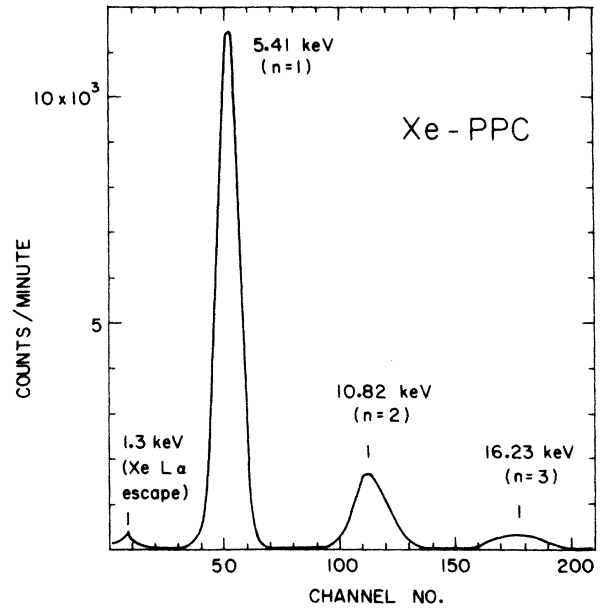

FIG. 8. Spectrum of transmitted Cr $K\alpha$ beam, recorded with a 5-cm-diam Xe-filled proportional counter. The $n=2$ and $n=3$ components have been relatively enhanced by absorbers; their intensity in the primary beam is 0.10 and 0.03% of the $n=1$ component, respectively. Background has been subtracted; the peak-to-background ratio is 250;1 at 5.41 keV. Zero of the energy scale is channel −10. Counting time was 40 min. The empirically determined correction factor for coincidence loss in the Xe counter is 1.02 at this counting rate.

are no longer radial, but tilted toward the end walls, when the field-tube voltage exceeds its ideal value.

4. *Measurement of integrated x-ray beam intensity*

Monitoring of the x-ray beam flux is somewhat complicated because the intensity is too high for direct counting. To guard against systematic errors in this critical aspect of the experiment, two alternative approaches were taken.

In monitoring arrangement A, illustrated in part of Fig. 5, and 0.004-mm-thick foil is placed at ~32° to the beam axis.[19] The material of the foil is such that its K binding energy lies just below the beam energy, i.e., Ti for Cr $K\alpha$ and Ni for W $L\alpha$ x rays.[21] Fluorescent radiation is detected at 90° to the beam with a xenon-filled proportional counter.[22] The system is calibrated at low flux with the aid of a second xenon proportional counter placed in the direct beam beyond the foil. Attenuation by the inclined foil is determined experimentally and accounted for. The monitor chamber is filled with helium. Calculated backscatter from the monitor foil into the active volume of the H_2 proportional counter is $< 10^{-5}$ of the x-ray beam intensity.

In an alternative arrangement B, the x-ray beam is attenuated with calibrated aluminum absorber foils and counted with a scintillation or proportional counter. The scintillation detector consists of a 1-mm-thick by 2.5-cm-diam cleaved Harshaw NaI(Tl) crystal mounted on an Amperex

XP-1010 photomultiplier tube. A typical spectrum from this detector is reproduced in Fig. 7(b). In many runs the scintillation detector was replaced by a xenon-filled proportional counter,[22] characterized by better resolution and lower background (Fig. 8).

With either monitoring arrangement, the number of x-ray photons that traverse the active region of the hydrogen proportional counter during a run is deduced from the number of counts recorded in the relevant portion of the background-corrected monitor-counter spectrum. Account is taken of the calibrated sampling efficiency of the monitoring device, of dead-time losses in the counter and electronics, and absorption in material encountered by the x rays between the edge of the active volume and the monitor counter.

Accurate determination of the sampling efficiencies of the beam monitoring arrangements requires accurate foil absorption measurements—of the single foil in arrangement A and of each of the two to four aluminum absorbers in B. These measurements were made by the "foil-in–foil-out" technique. Account was taken of the effect of the dead time τ of counter and electronics. Let the measured foil absorption factor R be the ratio of the measured counting rate N_0 (with the foil out of the beam) to the measured counting rate N_1 (with the foil in the beam). In each case the "true" counting rate is $N(1-\tau N)^{-1}$. The dead time of the counting apparatus was measured and its effect accounted for by a simple method due to Chipman[23]: The factor R is measured for various beam intensities and plotted as a function of N_0. The slope of a straight line fitted to the data points is then $\tau(1-R_{\text{true}})$, and the zero-count-rate intercept is R_{true}.

III. RESULTS

Twenty-five runs were made under varying conditions, as detailed in Table I. Errors listed for the results of individual runs are systematic errors, computed from the following uncertainties[24] for measurements at 5.4 keV: 2.53% in the length of the active counter volume, 0.50% in the gas pressure, 0.34% in the temperature, from 0.01 to 0.25% in foil absorption (monitoring method B), 1.74% in the correction for absorption by the H_2-chamber Be exit window, 1.40% in absorption by the detector Be window, from 0.16 to 0.68% in the air-scattering correction at the beam-flux monitor, from 0.23 to 1.70% in the analysis of the H_2 proportional-counter spectrum, and from 0.04 to 0.16% in the analysis of the beam-monitor spectrum. The same uncertainties apply to the 8.4-keV measurements, with the following exceptions: Uncertainties in foil absorption for monitoring method B ranged from 0.28 to 1.09% of the absorption factor for each foil; uncertainties in the correction for absorption by the H_2 and monitor-counter Be windows were 0.81 and 0.58%, respectively; the air-scattering correction was known to within 0.18%, but the uncertainties in the analysis of the H_2 photoelectron spectrum ranged from 1.03 to 2.70% of the total number of photoelectric events; and the uncertainty in the analysis of the beam-monitor spectrum was between 0.10 and 0.22%. The errors stated in the "final result" lines of Table I are the sum of the average systematic error (2.4 mb/atom at 5.4 keV) and of the standard deviation (0.5 mb/atom at 5.4 keV).

IV. DISCUSSION

It is interesting to compare the present experimental results with theoretical predictions. The nonrelativistic differential photoelectric cross section for hydrogen *atoms* has been derived by Heitler[25] through perturbation theory. With a plane wave for the continuum state (Born approximation), the result is

$$\sigma_{H_1} = 32(137)^3 \sigma_T (I/k)^{7/2}, \tag{1}$$

where I is the ionization energy, $\sigma_T = (8\pi/3)(e^2/mc^2)^2$ is the Thomson cross section, and k is the energy of the incident photon divided by $\hbar c$. If a Coulomb wave function is used to describe the ejected electron,[25,26] rather than a plane wave, the following result is found for the photoelectric cross section of atomic hydrogen:

$$\sigma_{H_1} = 64\pi(137)^3 \left(\frac{I}{k}\right)^4 \frac{e^{-4\xi \operatorname{cotan}^{-1}\xi}}{1-e^{-2\pi\xi}} \times \sigma_T, \tag{2}$$

where $\xi = [I/(k-I)]^{1/2}$.

The result of a relativistic calculation of the photoelectric cross section of atomic hydrogen has been reported by McCrary, Looney, and Atwater[5] for the photon energy 5.9 keV. These workers used a modified version of a method due to Brysk and Zerby,[27] with a bound-state wave function from a relativistic Dirac-Slater self-consistent field program.[28] Most recently, Scofield[29] has performed extensive relativistic Hartree-Slater calculations of photoionization cross sections. As can be seen from Table II, the cross sections calculated by McCrary *et al.*[5] and by Scofield[29] are very close to the nonrelativistic value obtained with a Coulomb final-state wave function.

The rather remarkable result of the present measurements is that the photoelectric cross section of the hydrogen molecule exceeds that of two

TABLE I. Summary of H_2 photoelectric cross-section measurements.

Run No.	Duration (min)	Pressure (atm H_2)	Mode[a]	Beam flux monitor[b]	Beam flux detectors[c]	Result[d] (mb/atom)
			5.41-keV Cr $K\alpha$ x rays			
1	40	2	I	A	scin-scin	55.80 ± 5.58
2	40	2	I	A	Xe-scin	55.10 ± 4.41
3	40	1	F	B	Xe	56.41 ± 1.98
4	20	1	F	B	Xe	55.45 ± 1.96
5	10	1	F	B	Xe	55.07 ± 1.97
6	10	1	F	B	Xe	54.24 ± 1.95
7	20	1	F	B	Xe	55.14 ± 1.94
8	20	1	F	B	Xe	53.33 ± 1.87
9	40	1	F	B	Xe	52.34 ± 1.90
10	20	1	F	B	Xe	52.51 ± 1.84
11	20	1	F	B	Xe	54.26 ± 1.84
12	40	1	F	B	Xe	52.45 ± 1.83
13	10	1	F	B	Xe	54.48 ± 1.91
14	10	1	F	B	scin	52.33 ± 2.79
15	10	1	F	B	scin	53.33 ± 2.85
16	10	1	F	B	Xe	52.58 ± 1.85
17	10	1	F	B	Xe	54.32 ± 1.91
Final result						54.0 ± 2.9
			8.39-keV W $L\alpha$ x rays			
1	100	1	F	B	Xe	12.25 ± 0.43
2	100	1	F	B	Xe	12.50 ± 0.43
3	400	1	F	B	Xe	12.17 ± 0.39
4	400	1	F	B	Xe	12.15 ± 0.42
5	100	1	I	B	Xe	11.67 ± 0.41
6	100	1	I	B	Xe	11.84 ± 0.41
7	200	1	F	B	Xe	12.47 ± 0.43
8	200	2	I	A	Xe-Xe	11.50 ± 0.61
Final result						12.0 ± 0.6

[a] F: continous H_2 flow. I: H_2 chamber isolated.
[b] See Sec. II C 4 for description of monitoring arrangements.
[c] Scin: scintillation spectrometer. Xe: xenon-filled proportional counter (Sec. II C 4).
[d] Errors estimated as described in Sec. III.

TABLE II. Hydrogen photoelectric cross sections (in mb/atom).

Photon energy (keV)	H_1 Heitler[a]	H_1 Heitler[b]	H_1 McCrary[c]	H_1 Scofield[d]	H_2 Kaplan and Markin[e] σ^+	H_2 Kaplan and Markin[e] σ^-	H_2 Experiment[f]
4		105.04		105.25	175	13	
5		48.99		49.07	85	6	
5.41	43.59	37.40		37.5*	64	4	54.0 ± 2.9
5.895		27.87	28.11				
8.39		8.29		8.34*			12.0 ± 0.6

[a] According to Ref. 25, Born approximation.
[b] According to Ref. 25, with exact Coulomb wave function for the free electron.
[c] Reference 5.
[d] Reference 29. Interpolated values are identified by asterisks.
[e] Reference 32. Here σ^+ corresponds to formation of the H_2^+ ion in the lowest electronic state, and σ^- to its formation in the repulsive electronic state. The total photoionization cross section is $\sigma^+ + \sigma^-$. Values for 5.41 keV were derived by extrapolation from results in Ref. 32.
[f] Present work.

hydrogen atoms by 44% at 5.4 keV and by essentially the same amount at 8.4 keV. This result should be considered in conjunction with that of measurements by Henke, Elgin, Lent, and Ledingham,[4] who found an excess of 60–70% of the H_2 cross section, measured by absorption, over twice the calculated H_1 photoionization cross section between 109 and 393 eV. (At these latter energies, the total cross section is virtually all photoelectric, and some six orders of magnitude larger than in the energy range of the present measurements, so that accurate photoelectric cross sections can be determined by careful absorption measurements.)

Very little theoretical work has been done on the photoionization of molecules. Cohen and Fano[30] have considered interference effects in the cross section at low energies. Flannery and Öpik[31] have treated the photoionization of the hydrogen molecule from the ground electronic and vibrational states, over the energy range from threshold (15.4 eV for a rotationless initial state) to 28 eV. The only calculations of which we are aware of the photoelectric cross sections of H_2 molecules for higher photon energies are due to Kaplan and Markin,[32] who cover the range from 80 eV to 5 keV. These workers describe the initial ground state of the H_2 molecule by a wave function which takes account of both the covalent and ionic aspects. They compute two cross sections: σ^+ for the formation of an H_2^+ ion in the lowest electronic state (threshold 15.4 eV) with a wave function proportional to $\phi_a + \phi_b$ (where ϕ_a and ϕ_b are the Slater 1*s* orbitals centered on atoms *a* and *b*, respectively), and the cross section σ^- for formation of the H_2^+ ion is the repulsive electronic state, with a wave function $\propto(\phi_a - \phi_b)$ and ionization potential 32.9 eV.[33] The emitted electron is described by a plane wave.

Some of the numerical results of Kaplan and Markin are included in Table II, as well as extrapolations to 5.4 keV. It is noteworthy that Kaplan and Markin's theoretical photoionization cross sections, per atom, for the H_2 molecule exceed calculated atomic cross sections by an amount roughly comparable to that found experimentally: Kaplan and Markin's total H_2 photoelectric cross section, $\sigma^+ + \sigma^-$, extrapolated to 5.4 keV, is 68 mb/atom. The H_1 atomic photoelectric cross section is lowered if a Coulomb wave function is used to describe the free electron, instead of a plane wave; the theoretical molecular cross section may also decrease if this refinement is introduced in the calculation. We are testing this hypothesis. The basic mechanism for the increased H_2 cross section may well be due to the greater charge density near each nucleus, compared with H_1, as has been pointed out by Fano.[34]

The effect of molecular bonding on the photoelectric cross section, even far above threshold, clearly calls for further exploration. We are extending this investigation to other energies and other low-*Z* substances.

ACKNOWLEDGMENTS

One of the authors (B.C.) is much indebted to Hans Mark, R. E. Price, and C. D. Swift for many helpful discussions on the planning of the experiment, and to Eugene Goldberg, Leader of E Division, Lawrence Livermore Laboratory, for his hospitality at the Laboratory and his interest in this work. We are grateful for the loan of apparatus built at the Lawrence Livermore Laboratory, where the special proportional counter was constructed with much skill and patience by Don Hirzel and Curt Rowe. We wish to thank J. W. Cooper and J. H. Hubbell of the National Bureau of Standards for instructive correspondence. R. W. Aman, A. J. Mord, Tomaž Rupnik, and D. K. McDaniels have lent helpful advice during various stages of the work.

---

*Work supported in part by the U. S. Army Research Office–Durham and by the U. S. Atomic Energy Commission.

†Present address: Department of Physics, Delta College, University Center, Mich. 48710.

[1]R. H. Messner, Z. Phys. 85, 727 (1933).

[2]S. J. M. Allen, quoted by A. H. Compton and S. K. Allison [*X-Rays in Theory and Experiment* (Van Nostrand, New York, 1935), 2nd ed., p. 799].

[3]A. J. Bearden, J. Appl. Phys. 37, 1681 (1966).

[4]B. L. Henke, R. L. Elgin, R. E. Lent, and R. B. Ledingham, Norelco Reporter 14, 112 (1967).

[5]J. H. McCrary, L. D. Looney, and H. F. Atwater, J. Appl. Phys. 41, 3570 (1970).

[6]T. M. Hahn, Phys. Rev. 46, 149 (1934).

[7]R. B. Roof, Jr., Phys. Rev. 113, 826 (1959).

[8](a) W. J. Veigele, E. Briggs, B. Bracewell, and M. Donaldson, X-Ray Cross Section Compilation, Kaman Nuclear Report No. KN-798-69-2(R), 1969 (unpublished); (b) W. J. Veigele, E. Briggs, L. Bates, E. M. Henry, and B. Bracewell, Kaman Sciences Corportation Report No. KN-71-431(R), 1971 (unpublished).

[9](a) E. Storm and H. I. Israel, Los Alamos Scientific Laboratory Report No. LA-3753, 1967 (unpublished); (b) Nucl. Data Tables A7, 565 (1970).

[10]W. H. McMaster, N. Kerr Del Grande, J. H. Mallett, and J. H. Hubbell, Compilation of X-Ray Cross Sections, Lawrence Radiation Laboratory Report No.

UCRL-50174, Sec. II Rev. 1, 1969 (unpublished).
[11]E. F. Plechaty and J. R. Terrall, Photon Cross Sections 1 keV to 100 MeV, Lawrence Radiation Laboratory Report No. UCRL-50400, Vol. VI, 1968 (unpublished).
[12]R. J. Grader, R. W. Hill, F. D. Seward, and A. Toor, Science 152, 1499 (1966); F. D. Seward (private communication).
[13]K. L. Bell and A. E. Kingston, Mon. Not. R. Astr. Soc. 136, 241 (1967).
[14]R. L. Brown and R. J. Gould, Phys. Rev. D 1, 2252 (1970).
[15]J. E. Felten and R. J. Gould, Phys. Rev. Lett. 17, 401 (1966).
[16]A. L. Cockroft and S. C. Curran, Rev. Sci. Instr. 22, 37 (1951).
[17]Matheson Gas Products, Newark, Calif. 94560; Airco Industrial Gases, City of Industry, Calif. 91746.
[18]J. R. Young, Rev. Sci. Instr. 34, 891 (1963).
[19]P. E. Koblas, Ph.D. thesis (University of Oregon, 1971) (unpublished).
[20]A. N. Prasad and J. D. Craggs, in *Atomic and Molecular Processes,* edited by D. R. Bates (Academic, New York, 1962), p. 206.
[21]Foils supplied by Goodfellow Metals Ltd., Claygate-Esher, Surrey, England.
[22]Reuter-Stokes, Cleveland, Ohio 44128.
[23]D. R. Chipman, Acta Crystallogr. A 25, 209 (1969).
[24]P. R. Bevington, *Data Reduction and Error Analysis for the Physical Sciences* (McGraw-Hill, New York, 1969).
[25]W. Heitler, *The Quantum Theory of Radiation* (Oxford U. P., Clarendon, England, 1954), 3rd ed., Sec. 21.
[26]M. Stobbe, Ann. Phys. 7, 661 (1930).
[27]H. Brysk and C. D. Zerby, Phys. Rev. 171, 292 (1968).
[28]D. Liberman, J. T. Waber, and D. T. Cromer, Phys. Rev. 137, A27 (1965).
[29]J. H. Scofield, Lawrence Livermore Laboratory Report No. UCRL-51326, 1973 (unpublished).
[30]H. D. Cohen and U. Fano, Phys. Rev. 150, 30 (1966).
[31]M. R. Flannery and U. Öpik, Proc. Phys. Soc. Lond. 86, 491 (1965).
[32]I. G. Kaplan and A. P. Markin, Dokl. Akad. Nauk SSSR 184, 66 (1969) [Sov. Phys.—Doklady 14, 36 (1969)]. For a recent extension of these calculations to 1 MeV, including relativistic effects, see I. G. Kaplan and A. P. Markin, Zh. Eksp. Teor. Fiz. 64, 424 (1973).
[33]D. R. Bates, U. Öpik, and G. Poots, Proc. Phys. Soc. Lond. A 66, 1113 (1953).
[34]J. W. Cooper (private communication).

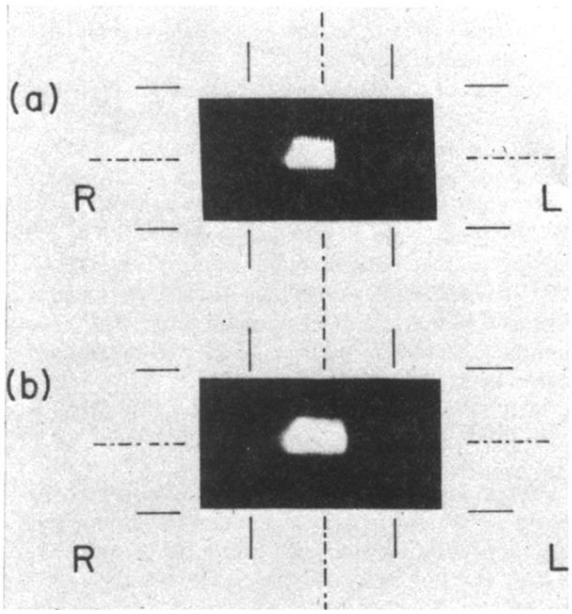

FIG. 6. Images of collimated Cr $K\alpha$ x-ray beam, (a) at entrance window and (b) at exit window of hydrogen chamber. Polaroid Type 57 film was exposed for (a) 210 min and (b) 240 min. Position of the edges of the 2.54-cm-diam beryllium windows is indicated by solid lines; the dot-dash lines intersect at the window centers.